

QM/MM Study of the Structure, Energy Storage, and Origin of the Bathochromic Shift in Vertebrate and Invertebrate Bathorhodopsins

Sivakumar Sekharan^{*,†} and Keiji Morokuma^{*,†,‡}

[†]Cherry L. Emerson Center for Scientific Computation and Department of Chemistry, Emory University, Atlanta, Georgia 30322, United States

[‡]Fukui Institute for Fundamental Chemistry, Kyoto University, 34-4 Takano Nishihiraki-cho, Kyoto 606-8103, Japan

S Supporting Information

ABSTRACT: By comparing the results from a hybrid quantum mechanics/molecular mechanics method (SORCI+Q//B3LYP/6-31G*:Amber) between vertebrate (bovine) and invertebrate (squid) visual pigments, the mechanism of molecular rearrangements, energy storage, and origin of the bathochromic shift accompanying the transformation of rhodopsin to bathorhodopsin have been evaluated. The analysis reveals that, in the presence of an unrelaxed binding site, bathorhodopsin was found to carry almost 27 kcal/mol energy in both visual pigments and absorb (λ_{max}) at 528 nm in bovine and 554 nm in squid. However, when the residues within 4.0 Å radius of the retinal are relaxed during the isomerization event, almost ~16 kcal/mol energy is lost in squid compared to only ~8 kcal/mol in bovine. Loss of a larger amount of energy in squid is attributed to the presence of a *flexible* binding site compared to a *rigid* binding site in bovine. Structure of the squid bathorhodopsin is characterized by formation of a direct H-bond between the Schiff base and Asn87.

Rhodopsin, the photoreceptor responsible for twilight vision in vertebrate and invertebrate species, belongs to the family of G-protein-coupled receptors, the largest family of cell surface receptors, with a known X-ray structure. It is composed of seven-transmembrane α -helices and contains the 11-*cis*-retinal chromophore attached to the ϵ -amino group of lysine residue through a protonated Schiff base (PSB11) linkage (Figure 1). Excitation by the visible light initiates 11-*cis* to 11-*trans* isomerization leading to the formation of bathorhodopsin.¹

In bovine (vertebrate) rhodopsin, which absorbs at 498 nm (57.4 kcal/mol), its batho intermediate was found to carry 35 ± 2 kcal/mol of energy and peak at ~535 nm.^{2–4} The energy stored is used to drive the protein through the visual cycle. Increased charge separation between PSBT and counterion (Glu113) upon photoisomerization⁵ and conformational distortion of the strained photointermediate⁶ were proposed as the major sources of energy storage; a 40:60 ratio of the two mechanisms was estimated on the basis of semiempirical calculations.⁷

Gascon used the ONIOM QM/MM-EE scheme at B3LYP/6-31G*:Amber//TDB3LYP level of theory to predict a batho model that carries 34.1 kcal/mol and absorbs at 485 nm.⁸ Andruniow used the multiconfigurational quantum chemical (CASPT2//CASSCF/6-31G*:Amber) treatment to predict a batho model that carries 26.0 kcal/mol and absorbs at 502 nm.⁹

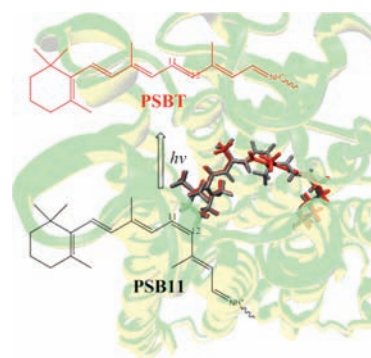


Figure 1. Photoisomerization of the protonated Schiff base of 11-*cis*-retinal chromophore (PSB11) to 11-*trans*-retinal chromophore (PSBT). Also shown in the background are the PSB11 (black) and PSBT (red) chromophores embedded into the seven-transmembrane α -helices of squid rhodopsin (yellow) and bathorhodopsin (green).

Both calculations ruled out a dominant role for charge separation between the PSBR and counterion in the energy storage process. The former attributed 50% of the energy to be stored in the form of electrostatic contribution,⁸ while the latter attributed the same amount to conformational distortion,⁹ supporting the conclusions originally reached by Röhrig.¹⁰ Irrespective of the method used, the calculations did not reproduce the red-shift of ~45 nm that serves as the signature motif of bathorhodopsin.¹¹

The X-ray structure of bovine bathorhodopsin became available around this time,¹² allowing a quantitative assessment of these factors using high-level quantum mechanical studies. Schrieber found an almost quantitative agreement with the spectra by calculating a red-shift of 36 nm (492→528 nm), but surprisingly only 16.3 kcal/mol was accounted for in that study.¹³ Khrenova modeled the ground-state reaction route from rho to batho and calculated only 16.0 kcal/mol and a 4-nm red-shift (515→519 nm).¹⁴ By using 9-demethyl analogue, Sugihara found Tyr191 and Tyr268 residues to stabilize the batho geometry,¹⁵ while Sekharan showed wat2a and wat2b to contribute a meager 2 kcal/mol toward the energy storage process.¹⁶ Despite numerous efforts, theoretical prediction of a batho model that accounts for both the energy storage and bathochromic shift has so far remained elusive.

Received: January 13, 2011

Published: March 10, 2011

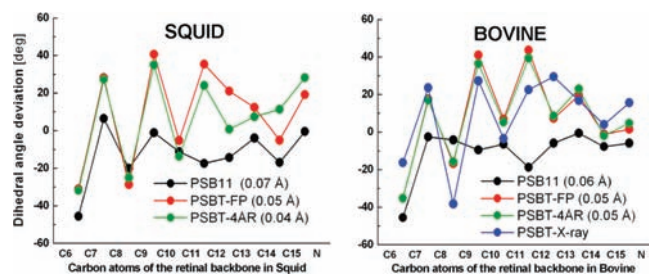


Figure 2. Dihedral angle deviations along the conjugated carbon chain of the retinal backbone atoms of bovine and squid rhodopsins. The deviations are from either *cis* (0°) or *trans* (180°) configuration. Refer to text for abbreviations. Values in parentheses indicate the bond length alternation of the chromophores discussed in this study. PSBT-X-ray in blue refers to the 2.6 \AA X-ray structure of bovine bathorhodopsin (PDB 2G87).

Recently, the X-ray structure of squid rhodopsin has opened the way for studying the primary event in vision in an invertebrate.^{17,18} Most earlier studies on invertebrate visual pigments were performed on octopus rhodopsin,¹⁹ and only a few studies were performed on squid rhodopsin, which showed the batho intermediate to peak at 550 nm , slightly more red-shifted than its vertebrate counterpart.²⁰

Since the mechanism of isomerization is an efficient, ultrafast, and stereoselective reaction, it is usually assumed that relaxation of the protein environment cannot occur within the experimentally observed 200-fs time frame.²¹ Furthermore, it is generally agreed that activation of rhodopsin by light and/or heat should follow the same molecular route²² and that the isomerization coordinate is mainly coupled to the vibrational modes of retinal.²³ These assumptions lead to the exclusion of protein relaxation in the ensuing QM/MM calculations of the primary event in visual²⁴ and archaeal rhodopsins.²⁵

In the present theoretical study, by taking bovine and squid rhodopsin structures as templates, we try to gain insights into structural rearrangements, energy uptake, and change in electronic spectra during *cis/trans* isomerization. We show that geometry relaxation of the protein environment in the vicinity of chromophore is essential for evaluating the photoisomerization process and accompanying spectral and energy changes.

We have attempted to obtain the structure of bathorhodopsin from bovine and squid rhodopsins using two sets of calculations that differ in the treatment of the binding site. To begin with, the QM/MM optimized structures of wild-type bovine and squid rhodopsins are taken from refs 26a and 26b. We first generate the relaxed intermediate structures along the ground-state minimum energy path ($S_0\text{-MEP}$), subject to the constraints of a fixed dihedral angle $\varphi(\text{C11}=\text{C12})$ about the isomerizing double bond. Geometry optimization is performed at the ONIOM-EE (B3LYP/6-31G*:Amber) level of theory implemented in Gaussian03²⁷ by incrementally rotating the $\text{C11}=\text{C12}$ dihedral angle from -17° in PSB11 (wild-type) to -180° . The resulting chromophores are then relaxed without any constraints in the dihedral angle yielding PSBT-FP, which corresponds to the structure obtained in the presence of a fixed protein (FP) environment, and PSBT-4 ÅR, which corresponds to the structure obtained when the residues within 4.0 \AA radius (4 \AA R) of any atom from the retinal are relaxed during the isomerization event. Such an approach allows us to gain insights into the influence of local environmental perturbations in the formation of bathorhodopsin. To obtain the electronic spectra, ab initio multireference QM/MM calculations

were performed on the resulting structures using the spectroscopy oriented configuration interaction (SORCI+Q)²⁸ method with 6-31G* basis using the ORCA 2.6.19 program.

In the absence of X-ray structure, the calculated geometric parameters of invertebrate bathorhodopsin are validated against its vertebrate counterpart resolved at 2.6 \AA resolution (PDB 2G87).¹² Average bond length alternation (BLA) of the C5–N moiety (Figure 2), defined as the average of the bond lengths of single bonds minus that of double bonds, is only slightly different for PSB11 in both pigments. Irrespective of the difference in the protein environments, the PSBT-FP geometry of bathorhodopsin contains a distorted chromophore with BLA 0.05 \AA . When the residues within 4.0 \AA radius are relaxed, distortion of the PSBT-4 ÅR geometry increases, and BLA decreases to 0.04 \AA in squid but not in bovine, indicating that significant perturbation of the local environment has taken place in the invertebrate pigment (Figure 2, top).

In the case of bovine bathorhodopsin, compared to the X-ray structure, the calculated bond angles differ by $\sim 5^\circ$ for the odd numbered carbon positions. Except for the terminal $\text{C15}=\text{N}$ bond, the dihedral angle deviations (Figure 2, bottom) of all the double bonds are strongly twisted from $\sim 20^\circ$ ($\text{C7}=\text{C8}$ bond), to almost 40° for ($\text{C9}=\text{C10}$ and $\text{C11}=\text{C12}$ bonds) in both pigments consistent with the resonance Raman²⁹ and NMR³⁰ spectroscopic measurements. Especially, a large twist ($\sim 20^\circ$) about the $\text{C13}=\text{C14}$ bond in bovine is found to be in good agreement with the X-ray structure.¹² A discrepancy is noted for the $\text{C12}=\text{C13}$ bond, which is found to be twisted in the X-ray structure. All the single bonds remain almost planar in good agreement with structures obtained from the related MEP calculations^{8,9} and molecular dynamics simulations.^{10,31} It is generally agreed that twisting of the chromophore in bovine rhodopsin is due to the presence of an H-bonding Glu113 counterion, which anchors the proton at the SB terminal and induces stiffness into the retinal backbone.^{32–34} Structural manifestation of the presence of a non-H-bond Glu180 counterion near the isomerizing $\text{C11}=\text{C12}$ in squid rhodopsin is seen in the dihedral angle deviations from C11 to SBN^+ moiety.

In bovine rhodopsin, the position of the Glu113 counterion remains almost unperturbed during the isomerization process, indicating a strong H-bonding strength for the SB.³⁵ In contrast, when the binding site is relaxed, distance between the SB and counterion (Glu180) in squid rhodopsin increases by 0.41 \AA (4.29 to 4.70 \AA). An increase in charge separation by $\sim 0.4 \text{ \AA}$ can be compared to the experimentally determined distance between the SB and the counterion (Glu113) in bovine bathorhodopsin, which increases by $\sim 0.45 \text{ \AA}$, from 3.45 to 3.88 \AA (chain A) or 3.28 to 3.74 \AA (chain B).¹² Also, Asn87 is drawn closer by almost 1.0 \AA (from 3.93 to 2.96 \AA) to form a strong H-bond with SB and Tyr111 by 0.16 \AA (from 3.41 to 3.25 \AA). This observation strongly argues against the popular notion that the protein structure remains frozen during the isomerization event and the X-ray structure of bathorhodopsin should correspond to the relaxed protein geometry in the vicinity of the chromophore.

One end of the retinal tether is held fixed by the β -ionone ring in the hydrophobic cleft of the binding site and the other end is bound to the protein via the SB-lysine linkage. Thus the $\text{C11}=\text{C12}$ bond undergoes a clockwise rotation from -17° in PSB11 to -136° – -145° in PSBT-FP geometry and to -141° – -156° in PSBT-4 ÅR geometry of bovine/squid bathorhodopsins. Experimental evidence for the distorted 11-*trans*-geometry is seen in the hydrogen out-of-plane wagging

modes at C11 and C12 positions³⁶ as the chromophore adopts a corkscrew-like structure with a right-hand screw sense.¹³ As a result, the *cis* link is shifted from the C11=C12 bond in rhodopsin to the C15=N bond in bathorhodopsin as originally proposed by Warshel³⁷ and recently validated by molecular dynamics simulations.³⁸ Therefore, irrespective of the change in position of the counterion, the chromophore should undergo isomerization via the “bicycle-pedal motion” in both visual pigments.

Comparison of the optimized geometries in vacuo shows the PSB11 to be less stable than the *trans*-isomer by 5.64 kcal/mol as a consequence of steric crowding around the *cis*-configured C11=C12 bond. However, results from the QM/MM calculation of the visual pigment reveal a different picture. Perusal of the QM and MM energies (see the Supporting Information) show that PSBT suffers significantly more destabilization that raises its energy and reverses the stability above that of the *cis*-isomer. As a consequence, the PSBT-FP model of squid bathorhodopsin was found to carry 27.60 kcal/mol energy, of which 14.03 kcal/mol (51%) is stored in the form of conformational distortion of the chromophore and the remaining 13.57 kcal/mol (49%) stems from the electrostatic and polarization effect of the fixed protein environment. The PSBT-FP model of bovine bathorhodopsin stores almost the same amount of energy (26.10 kcal/mol), of which 19.78 kcal/mol (75%) is attributed to conformational distortion and only 6.32 kcal/mol (25%) is due to the electrostatic and polarization effect. The calculated value of 26.10 kcal/mol is in excellent agreement with the Arrhenius activation energy²³ of ~ 25 kcal/mol and with the photocalorimetric measurements^{2,3} of 35 ± 2 kcal/mol for bovine rhodopsin.

The situation changes dramatically, more so for squid rhodopsin, when the immediate environment is relaxed during isomerization. The PSBT-4ÅR model of squid bathorhodopsin stores only 11.08 kcal/mol of energy, of which 1.99 kcal/mol (17%) is stored in the form of geometric distortion and 9.08 kcal/mol (83%) is retained via electrostatic and polarization effect. In contrast, the PSBT-4ÅR model of bovine bathorhodopsin stores almost 19.45 kcal/mol of energy, of which 15.58 kcal/mol (80%) is retained through geometric distortion and 3.87 kcal/mol (20%) via electrostatic and polarization effect. Apparently, the loss of a substantial amount of energy is attributed to the presence of a flexible binding site in squid (due to the non-H-bonding Glu180 counterion) compared to a rigid binding site in bovine rhodopsin (due to the H-bonding Glu113 counterion).³⁹

Because Glu181 occupies the position corresponding to Glu180 counterion in squid, the MEP calculations were performed in the presence of a charged Glu181 residue in bovine rhodopsin. Although Glu181 was postulated to be involved in the counterion-switch mechanism,⁴⁰ we find no role for a charged Glu181 residue in the energy storage process as long as the binding site remains unrelaxed, in agreement with Tomasello.⁴¹ When the binding site is relaxed in the presence of a charged Glu181 residue in bovine rhodopsin the energy stored is reduced by 3 kcal/mol, which indicates that Glu180 may have mediated the energy storage process in squid bathorhodopsin (see the potential energy curve around the φ (C11=C12) bond in the SI). Therefore, we suggest that, for optimum storage of the photonic energy required for driving the visual cycle, it is advantageous for the protein environment to remain almost unrelaxed during the photochemical event.

Now turning our attention to the UV/vis spectral data and how they develop as a function of the structural changes the

Table 1. Calculated SORCI+Q First Vertical Excited State ($S_1 \rightarrow S_0$) Absorption Wavelengths (λ , nm), Oscillator (f) and Rotatory Strengths (R , au), and Difference in the Ground (S_0)- and Excited (S_1)-State Dipole Moments ($\Delta\mu$) of the PSBR Chromophores in the Gas-Phase (QM-none) and Protein (QM/MM) Environments^a

PSBR	gas phase			protein			$\Delta\mu$
	λ	f	R	λ	f	R	
Bovine Rhodopsin and Bathorhodopsin							
PSB11	616	1.20	+0.09	495	1.40	+0.21	12.1
PSBT-FP	657	1.31	-0.98	528	1.43	-0.83	12.7
PSBT-4 ÅR	635	1.37	-0.96	525	1.50	-0.83	12.9
Squid Rhodopsin and Bathorhodopsin							
PSB11	604	0.93	+0.16	490	1.14	+0.32	11.7
PSBT-FP	677	1.12	-1.17	554	1.25	-1.08	12.2
PSBT-4 ÅR	649	1.29	-0.76	543	1.39	-0.72	12.7

^a Experimental values for bovine: PSB11 = 506 nm; PSBT = 543 nm; and squid: PSB11 = 493 nm; PSBT = 550 nm are taken from ref 20

chromophores undergo, we take a look at the SORCI+Q calculated ground- and the excited-state properties in Table 1. It has already been shown that both the 11-*cis* and 11-*trans* chromophores absorb at around 610 nm in vacuo and the difference between the calculated λ_{\max} of PSB11 and the PSBT chromophores is very small (~ 10 nm), probably too small to be detected experimentally.⁴²⁻⁴⁵

In contrast, irrespective of the treatment of the binding site, geometric distortions accumulated during the isomerization event decrease the BLA and shift the λ_{\max} from 616/604 nm to the red, 635/657 nm in bovine and 649/677 nm in squid. This indicates that origin of the bathochromic shift lies at geometric distortion of the PSBT chromophore. Interaction of the chromophore with counterion induces a strong blue-shift of ~ 100 nm and shifts the calculated λ_{\max} very close to the experimental values, 528/525 nm in bovine^{4,46} and 554/543 nm in squid bathorhodopsins.²⁰ The effect of the counterion is conceivable, as the excited-state charge density is shifted against the charge of the counterion. This shift is also the reason for the change in the dipole moment of the S_1 state relative to the S_0 state, calculated to be ~ 12.0 D in good agreement with the experimental observations (12.0 ± 2.0 D).⁴⁷ Compared to the strong blue-shift of the counterion, the spectral shifts from the neutral residues are negligible.⁴⁸ The increase in oscillator strength of the batho intermediate found in the experimental observations⁷ is also reproduced in the QM/MM calculations.

Absolute sense of the twist of the corkscrew-like structure of the bathorhodopsin chromophore is evaluated by calculating the rotatory strengths before and after isomerization. Out-of-plane distortion about the C11=C12 (negative) and C12-C13 (positive) bonds imparts a positive helicity on the rhodopsin chromophore, yielding a positive rotatory strength (R) in both pigments.⁴⁹ The respective calculated values for α -band and R of 495 nm and +0.21 au for bovine and 490 nm and +0.32 au for squid agree in sign and magnitude with the experimental values.⁵⁰ In bathorhodopsin, the band inverts in sign and magnitude with the R value of -0.83 au in bovine and -1.08 au in squid. Both the sign inversion and marked increase in the spectral gap of ~ 30 nm in bovine and ~ 50 nm in squid are already seen in their respective gas-phase spectra and are only slightly increased by their corresponding

protein environments. The small blue shift between the two rhodopsin pigments is attributed to the increase in BLA, ~ 0.06 Å in bovine to ~ 0.07 Å in squid,^{26,39} and the small red shift between the bathorhodopsin pigments can be traced back to the decrease in BLA, 0.05 Å in bovine to 0.04 Å in squid (Figure 2).

In conclusion, by taking the bovine and squid rhodopsin structures as templates, we have gained insights into the structural rearrangements, energy uptake, and change in electronic spectra during the *cis/trans* isomerization. QM/MM calculated models of bathorhodopsin explain the consequence of configurational change in the first step of visual excitation and reproduce the main experimental observations in both vertebrate and invertebrate pigments. From the evidence gathered, it is proposed that, similar to bovine rhodopsin, squid rhodopsin may also isomerize via the “bicycle-pedal motion” pathway. Thus, organisms everywhere may tend to gravitate toward a common solution even in an apparatus as intriguing as an eye.

■ ASSOCIATED CONTENT

S Supporting Information. Model building, Cartesian coordinates of retinal models, and complete references. This material is available free of charge via the Internet at <http://pubs.acs.org>.

■ AUTHOR INFORMATION

Corresponding Author

ssekhar@emory.edu; morokuma@emory.edu

■ ACKNOWLEDGMENT

We thank Profs. R. R. Birge, J. Gascon, and A. Cooper for the valuable discussions. The work at Emory is supported in part by a grant from the National Institutes of Health (R01EY016400-04) and at Kyoto by a Core Research for Evolutional Science and Technology (CREST) Grant in the area of High Performance Computing for Multiscale and Multiphysics Phenomena JST.

■ REFERENCES

- (1) Smith, S. O.; Courtin, J.; De Groot, H.; Gebhard, R.; Lugtenburg, J. *Biochemistry* **2001**, *30*, 7409–7415.
- (2) Cooper, A. *Nature* **1979**, *282*, 531–533.
- (3) Schick, G. A.; Cooper, T. M.; Holloway, R. A.; Murray, L. P.; Birge, R. R. *Biochemistry* **1987**, *26*, 2556–2562.
- (4) Kandori, H.; Shichida, Y.; Yoshizawa, T. *Biophys. J.* **1989**, *56*, 453–457.
- (5) Honig, B.; Ebrey, T.; Callender, R. H.; Dinur, U.; Ottolenghi, M. *Proc. Natl. Acad. Sci. U.S.A.* **1979**, *76*, 2503–2507.
- (6) Warshel, A.; Barbo, N. *J. Am. Chem. Soc.* **1982**, *104*, 1469–1476.
- (7) Birge, R. R.; Einterz, C. M.; Knapp, H. M.; Murray, L. P. *Biophys. J.* **1988**, *53*, 367–385.
- (8) Gascon, J. A.; Batista, V. S. *Biophys. J.* **2004**, *87*, 2931–2941.
- (9) Andruniow, T.; Ferrè, N.; Olivucci, M. *Proc. Natl. Acad. Sci. U.S.A.* **2004**, *101*, 17908–17913.
- (10) Röhrig, U. F.; Guidoni, L.; Laio, A.; Frank, I.; Rothlisberger, U. *J. Am. Chem. Soc.* **2004**, *126*, 15328–15329.
- (11) Einterz, C. M.; Lewis, J. W.; Kligler, D. S. *Proc. Natl. Acad. Sci. U.S.A.* **1987**, *84*, 3699–3703.
- (12) Nakamichi, H.; Okada, T. *Angew. Chem., Int. Ed.* **2006**, *45*, 4270–4273.
- (13) Schreiber, H.; Sugihara, M.; Okada, T.; Buss, V. *Angew. Chem., Int. Ed.* **2006**, *45*, 4274–4277.
- (14) Khrenova, M. G.; Bochenkova, A. V.; Nemukhin, A. V. *Proteins* **2009**, *78*, 614–622.
- (15) Sugihara, M.; Buss, V. *Biochemistry* **2008**, *47*, 13733–13735.
- (16) Sekharan, S. *Photochem. Photobiol.* **2009**, *85*, 517–520.
- (17) Shimamura, T.; et al. *J. Biol. Chem.* **2008**, *283*, 17753–17756.
- (18) Murakami, M.; Kouyama, T. *Nature* **2008**, *453*, 363–367.
- (19) Tsuda, M.; Tokunaga, F.; Ebrey, T. G.; Yue, K. T.; Marque, J.; Eiseinstein, L. *Nature* **1980**, *287*, 461–462.
- (20) Sulkes, M.; Lewis, A.; Marcus, M. A. *Biochemistry* **1978**, *17*, 4712–4722.
- (21) Kukura, P.; McCamant, D. W.; Yoon, S.; Wandschneider, D. B.; Mathies, R. A. *Science* **2005**, *310*, 1006–1009.
- (22) Ala-lauria, P.; Donner, C.; Koskelainen, A. *Biophys. J.* **2004**, *86*, 3653.
- (23) Lin, S. W.; Groesbeek, M.; van der Hoef, I.; Verdegem, P.; Lugtenburg, J.; Mathies, R. A. *J. Phys. Chem. B.* **1998**, *102*, 2787–2806.
- (24) Polli, D.; et al. *Nature* **2010**, *467*, 440–443.
- (25) Altoè, P.; Cembran, A.; Olivucci, M.; Garavelli, M. *Proc Natl Acad Sci U.S.A.* **2010**, *107*, 20172–20177.
- (26) (a) Altun, A.; Yokoyama, S.; Morokuma, S. *J. Phys. Chem. B* **2008**, *112*, 6814–6827. (b) Sekharan, S.; Altun, A.; Morokuma, K. *Chem.—Eur. J.* **2010**, *16*, 1744.
- (27) Frisch, M. J. et al. GAUSSIAN; Gaussian Inc.: Pittsburgh PA, 2003.
- (28) Neese, F. A. *J. Chem. Phys.* **2003**, *119*, 9428–9443.
- (29) Kim, J. E.; Pan, D.; Mathies, R. A. *Biochemistry* **2003**, *42*, 5169–5175.
- (30) Concistrè, M.; et al. *J. Am. Chem. Soc.* **2008**, *130*, 10490–10491.
- (31) Frutos, L. M.; Andruniów, T.; Santoro, F.; Ferrè, N.; Olivucci, M. *Proc Natl Acad Sci U.S.A.* **2007**, *2410*–2418.
- (32) Liu, R. S.; Asato, A. E. *Proc. Natl. Acad. Sci. U.S.A.* **1985**, *82*, 259–263.
- (33) Vergdegem, P. J. E.; Bovee-Geurts, P. H. M.; de Grip, W. J.; Lugtenburg, J.; de Groot, H. J. M. *Biochemistry* **1998**, *38*, 11316.
- (34) Sugihara, M.; Hufen, J.; Buss, V. *Biochemistry* **2006**, *45*, 801–810.
- (35) Ota, T.; Furutani, Y.; Terakita, A.; Yoshinori, S.; Kandori, H. *Biochemistry* **2006**, *45*, 2845–2851.
- (36) Palings, I.; van den Berg, E. M. M.; Lugtenburg, J.; Mathies, R. A. *Biochemistry* **1989**, *28*, 1498–1507.
- (37) Warshel, A. *Nature* **1976**, *260*, 679–683.
- (38) Schapiro, I.; Weingart, O.; Buss, V. *J. Am. Chem. Soc.* **2009**, *131*, 16–17.
- (39) Sekharan, S.; Altun, A.; Morokuma, K. *J. Am. Chem. Soc.* **2010**, *132*, 15856–15859.
- (40) Yan, E. C. Y.; et al. *Proc. Natl. Acad. Sci. U.S.A.* **2003**, *100*, 9262–9267.
- (41) Tomasello, G.; et al. *J. Am. Chem. Soc.* **2009**, *131*, 5172–5186.
- (42) Wanko, M.; et al. *J. Phys. Chem. B* **2005**, *109*, 3606–3615.
- (43) Nielsen, I. B.; Lammich, L.; Andersen, L. H. *Phys. Rev. Lett.* **2006**, *96*, 018304–018307.
- (44) Sekharan, S.; Weingart, O.; Buss, V. *Biophys. J.* **2006**, *91*, L07–L09.
- (45) Hoffmann, M.; et al. *J. Am. Chem. Soc.* **2006**, *128*, 10808–10818.
- (46) Spalink, J. D.; Reynolds, A. H.; Rentzepis, P. M.; Sperling, W.; Applebury, M. L. *Proc. Natl. Acad. Sci. U.S.A.* **1983**, *80*, 1887–189.
- (47) Mathies, R. A.; Styrrer, L. *Proc. Natl. Acad. Sci. U.S.A.* **1976**, *73*, 2169.
- (48) Sekharan, S.; Sugihara, M.; Buss, V. *Angew. Chem., Int. Ed.* **2007**, *46*, 269–271.
- (49) Buss, V.; Kolster, K.; Terstegen, F.; Vahrenhost, R. *Angew. Chem., Int. Ed.* **1998**, *37*, 1893–1895.
- (50) (a) Horiuchi, S.; Tokunaga, F.; Yoshizawa, T. *Biochim. Biophys. Acta* **1980**, *591*, 445–457. (b) Shichida, Y.; Tokunaga, F.; Yoshizawa, T. *Biochim. Biophys. Acta* **1978**, *504*, 413–430.